

# High-Pressure Phase Equilibria of Squalene + Carbon Dioxide: New Data and Thermodynamic Modeling

Elvis J. Hernández, F. Javier Señoráns, Guillermo Reglero, and Tiziana Fornari\*

Sección Departamental de Ciencias de la Alimentación, Universidad Autónoma de Madrid, Campus de Cantoblanco, 28049 Madrid, Spain

The importance of squalene in both the cosmetic and pharmaceutical industries motivated the development of new technologies to purify squalene from different sources, one of such technologies being the supercritical fluid extraction using carbon dioxide (CO<sub>2</sub>). Knowledge of phase equilibria behavior is essential for the design of these processes. In this work, vapor–liquid equilibria of the binary system squalene + CO<sub>2</sub> at high pressures (10 to 35) MPa and at  $T = (313, 323, \text{ and } 333)$  K were measured using a variable-volume view cell. Experimental compositions of both the liquid and vapor phases were compared with previous data available in the literature. Additionally, the results obtained in this work were employed to evaluate the capability of a group contribution based equation of state in the phase equilibria modeling of the squalene + CO<sub>2</sub> mixture.

## Introduction

Squalene (2,6,10,15,19,23-hexamethyl tetracosaeheptaene) is an important component of epidermis, protecting the skin surface from lipid peroxidation. Further, it was recognized that diet supplementation with squalene may reduce cholesterol and triglyceride levels in animals.<sup>1</sup> Thus, squalene might be a useful complement to promote the effects of some cholesterol-lowering drugs. Additionally, recent studies directed the therapeutic use of squalene in a variety of cancers.<sup>2</sup>

Several processes to purify squalene from different sources have been reported in the literature, such as molecular distillation, high-speed countercurrent chromatography, and countercurrent supercritical CO<sub>2</sub> extraction.<sup>3–8</sup>

The primary natural source of squalene is shark liver oil, but it can also be found as a minor constituent in olive oil. Thus, residues of the olive oil deodorization process are viable raw materials for the production of squalene from vegetal sources.

Regarding the squalene production using supercritical CO<sub>2</sub> technology, several works have been reported in the literature. The recovery of squalene from shark liver oil was studied by Catchpole et al.;<sup>3–7</sup> the concentration of squalene from olive oil deodorizer distillates was considered by Bondioli et al.;<sup>8</sup> and the purification of squalene from an ethylated olive oil deodorizer distillate was reported by Vázquez et al.<sup>9</sup> All works agreed on the feasibility of supercritical CO<sub>2</sub> technology to purify squalene from lipid-type raw materials. Simulation and optimization of these processes require knowledge of CO<sub>2</sub> + squalene phase equilibria data, as well as a thermodynamic tool capable of predicting phase compositions accurately. Previous data available in the literature are the measurements reported by Catchpole et al.<sup>4,5</sup> and Brunner et al.<sup>10</sup> Recently, Martínez-Correa et al.<sup>11</sup> reported new squalene solubility data and discussed the application of two well-known thermodynamic

models: the Peng–Robinson Equation of State and the Group Contribution Equation of State (GC-EoS).

In this work, vapor–liquid phase equilibria compositions of the binary system squalene + CO<sub>2</sub> at pressures ranging from (10 to 35) MPa and at  $T = (313, 323, \text{ and } 333)$  K were measured. Experiments were conducted by the static analytical method, using a high-pressure variable-volume cell. The experimental results obtained were compared with previous data available in the literature<sup>4,5,10,11</sup> and were represented using the GC-EoS model.

## Materials and Methods

**Chemicals.** Squalene, 98 % mass of purity according to seller specifications, was used in the present study and was obtained from Sigma-Aldrich (St. Louis, MO, USA). Carbon dioxide N38 (99.98 % mass) was purchased from AL Air Liquid España S. A. (Madrid, Spain).

**Equipment and Experimental Procedure.** Measurements were carried out by the static analytical method, using a high-pressure variable-volume cell (maximum capacity 120 cm<sup>3</sup>). A scheme of the experimental device employed is given in Figure 1. The equipment consists of a cylinder vessel with a front window and a piston, which is smoothly displaced inside the cylinder using a manual pressure generator. The cylinder is surrounded by a thick aluminum jacket, externally heated by two electrical resistances connected to a temperature controller. The uncertainty in the temperature measurement is  $\pm 0.1$  K. A gauge transducer coupled with a digital indicator provides the pressure measurements with an uncertainty of  $\pm 20$  kPa. A detailed explanation of the experimental device can be found elsewhere.<sup>12</sup>

Squalene was introduced into the cell, and it was purged with CO<sub>2</sub> at low pressure to remove the residual air. Then, CO<sub>2</sub> was allowed to flow into the cell. Once the temperature was stabilized, the desired pressure was achieved (by means of the manual pressure generator), and the magnetic stirrer was turned on. After 1.5 h, stirring was stopped, and the mixture was allowed to repose at least for 3 h in order that phase segregation

\* Corresponding author. Tel.: + 34 914972380. E-mail: tiziana.fornari@uam.es.

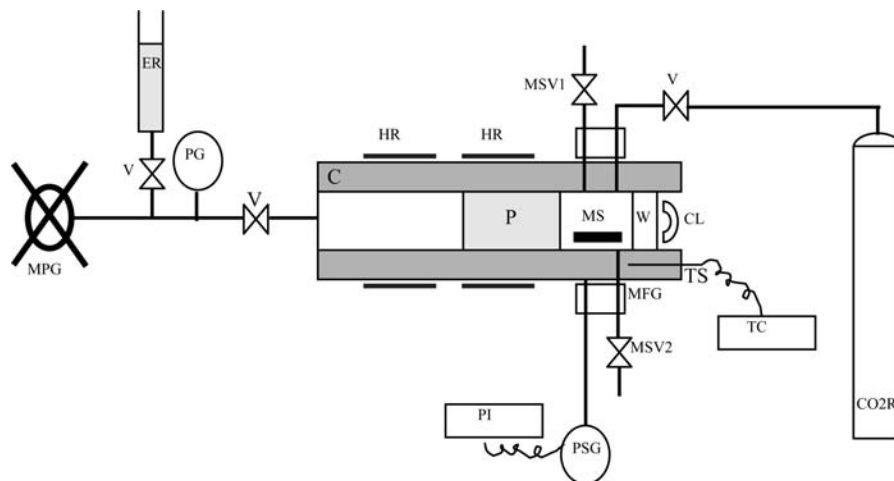


**Figure 1.** Scheme of the experimental device. C, variable-volume cell; P, piston; MPG, manual pressure generator; MS, magnetic stirrer; W, glass window; CL, cold light; HR, heating resistances; MFG, magnetic field generator; TS, temperature sensor; TC, temperature controller; PS, pressure sensor; PI, pressure indicator; ER, ethanol reservoir; CO2R, CO<sub>2</sub> reservoir; V, on-off valve; MSV1 and MSV2, micrometering sampling valves; PG, pressure gauge.

occurred. The frontal window with the cold end light was employed to visually verify the existence of two phases.

Samples from the top and bottom of the equilibrium cell were withdrawn using capillary lines and micrometering valves and decompressed to atmospheric pressure. Both valves were thermostated at the same temperature of the equilibrium cell. The manual pressure generator was employed to keep pressure constant during sampling ( $\pm 10$  kPa). Squalene was collected in glass vials and separated from the CO<sub>2</sub> by using a trap. Vials were weighed in a precision analytical balance with 0.0001 g accuracy (Denver Instrument Apx-60) to determine the amount of squalene. The amount of CO<sub>2</sub> was determined volumetrically using a 1000 mL graduated tube filled with a saturated solution of Na<sub>2</sub>SO<sub>4</sub> to prevent CO<sub>2</sub> dissolution. The volume of gas was quantified as the displaced liquid volume and corrected by accounting for the effects of temperature, atmospheric pressure, and water vapor pressure. All samples were collected by duplicate.

Typically 450 mL of CO<sub>2</sub> (ambient conditions) was withdrawn from the supercritical phase, and the mass of squalene collected in the glass vials was in the range from (1 to 100) mg. In the case of the liquid phase, (100 to 200) mL of CO<sub>2</sub> (ambient conditions) was withdrawn when sampling, and (200 to 1000) mg of squalene was recovered in the vials.

The uncertainty of the experimental CO<sub>2</sub> mass fractions ( $z_{\text{CO}_2}$ ) was calculated as the average standard deviation (ASD) between the values obtained

$$\text{ASD} = (1/2) \sqrt{(1/N_{\text{exp}}) \sum (z_{\text{CO}_2}^{\text{I}} - z_{\text{CO}_2}^{\text{II}})^2}$$

where I and II represent the duplicate experiments and  $N_{\text{exp}}$  is the number of data points. The calculated ASD values were 0.004 in the CO<sub>2</sub> liquid mass fraction and 0.008 in the case of the CO<sub>2</sub> mass fraction in the supercritical phase.

## Results and Discussion

**Experimental Results.** Table 1 shows the experimental vapor-liquid equilibria data obtained at the different conditions of temperature and pressure. As expected, both the solubility of squalene in the supercritical phase and the solubility of CO<sub>2</sub> in the liquid squalene-rich phase increase with pressure.

**Table 1.** Vapor-Liquid Equilibria Data Measured in this Work for the Binary System CO<sub>2</sub> (1) + Squalene (2)

$T$ K	$p$ MPa	$w_1$ (liquid phase)	$w_2$ (supercritical phase)
333	35	0.448	0.101
	30	0.369	0.054
	25	0.326	0.037
	20	0.272	0.023
	15	0.236	0.007
	10	0.177	-
323	35	0.388	0.093
	30	0.345	0.066
	25	0.318	0.045
	20	0.295	0.027
	15	0.271	0.011
	10	0.198	0.001
313	30	0.378	0.079
	25	0.305	0.054
	20	0.274	0.033
	15	0.253	0.016
	10	0.224	0.001

Figure 2 shows a general comparison between the squalene solubility data reported by different authors<sup>4,5,10,11</sup> and the new data measured in this work. Symbols in Figure 2 do not differentiate temperature but only the source of data (the experimental temperature range is given in the Figure 2 caption). As can be observed, our data compare qualitatively well with the rest of the data available. Particularly, in the high-pressure range, our data are more similar to the data reported by Brunner et al.<sup>9</sup> than to the solubility data given by Martínez-Correa et al.<sup>11</sup>

Figure 3 depicts the different squalene solubility data as a function of pressure and temperature. As can be observed in the different representations, all different sets of data show a weak dependence of solubility with temperature; at low pressure (< 25 MPa) solubility increases with decreasing temperature (due to the increase of CO<sub>2</sub> density), but crossover is observed in all cases at pressures higher than 25 MPa.

To give an order of magnitude of the discrepancies between the different sources of experimental data, the average relative deviations (ARD) between the phase compositions reported in the literature and the new data reported in this work are given in Table 2. Only the data obtained at exactly at the same temperature and pressure were considered; Table 2 reports the

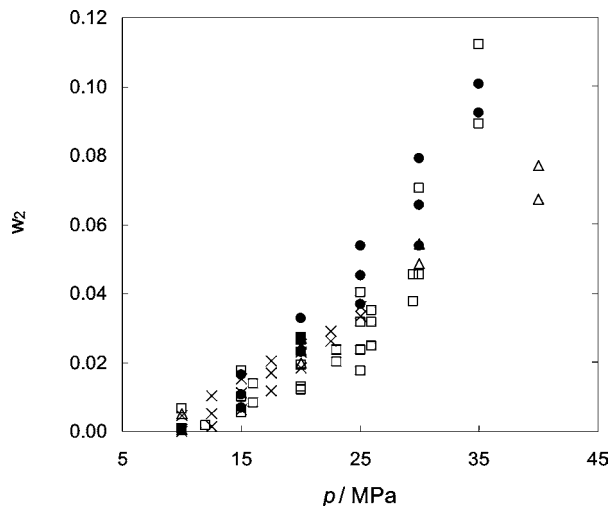


**Figure 2.** Squalene solubility  $w_2$  in supercritical  $\text{CO}_2$ : comparison between experimental data reported in the literature and the data measured in this work:  $\times$ , refs 4 and 5,  $T = (313 \text{ to } 323) \text{ K}$ ;  $\square$ , ref 10,  $T = (313 \text{ to } 373) \text{ K}$ ;  $\triangle$ , ref 11,  $T = (313 \text{ to } 323) \text{ K}$ ;  $\bullet$ , this work,  $T = (313 \text{ to } 333) \text{ K}$ .

calculated ARD values at 333 K. As can be deduced from the table, our data are more similar to the values reported by Brunner et al.<sup>10</sup> than those given by Catchpole et al.<sup>4,5</sup> Analogous conclusions can be established at the other temperatures. Similarly to our work, Brunner et al.<sup>10</sup> employed a closed equilibrium cell system, from which small amount of samples were withdrawn after the mixture attained the equilibrium

**Table 2.**  $\text{CO}_2$  (1) + Squalene (2) Phase Equilibria: Average Relative Deviations (ARD<sup>a</sup>) between the Phase Compositions Reported in the Literature and the New Data Reported in this Work at 333 K and Pressures from (10 to 35) MPa

ref	100 ARD ( $w_1$ )	100 ARD ( $w_2$ )
Catchpole et al. <sup>4,5</sup>	15.9	48.1
Brunner et al. <sup>9</sup>	6.4	27.1

<sup>a</sup> ARD =  $(1/N_{\text{exp}}) \sum |w_i^{\text{this work}} - w_i^{\text{ref}}| / w_i^{\text{this work}}$ ,  $N_{\text{exp}}$  being the number of experimental data points and  $w_i$  the mass fraction of  $\text{CO}_2$  in the liquid phase or the mass fraction of squalene in the supercritical phase.

conditions (in our experiments, 3 h was necessary to ensure a clear segregation of phases). Catchpole et al.<sup>4,5</sup> employed a countercurrent packed column device, which is not a common device utilized to carry out phase equilibria measurements; several sources of error can be identified, such as too small density difference between squalene and  $\text{CO}_2$ , insufficient squalene flow rate and/or packed height to achieve saturation, and variation of apparent solubility with  $\text{CO}_2$  flow rate.<sup>4</sup> The larger discrepancies of our data in comparison with the data reported by Catchpole et al.<sup>4,5</sup> can be attributed to the different type of experimental equipment employed.

**Thermodynamic Modeling.** The solubility of squalene in  $\text{SCCO}_2$  was represented in the literature using different approaches, such as simple empirical density based equations<sup>4,5,11</sup> or the Peng–Robinson EoS.<sup>4,11</sup> The modeling of the equilibrium composition of both the liquid and the supercritical phases was reported by Catchpole et al.,<sup>4</sup> applying the Peng–Robinson EoS and the Kwak and Mansoori mixing rule (PR-KM EoS), and by Brunner et al.<sup>10</sup> using the Soave–Redlich–Kwong EoS with the Mathias–Klotz–Prausnitz mixing rule (SRK-MKP EoS).

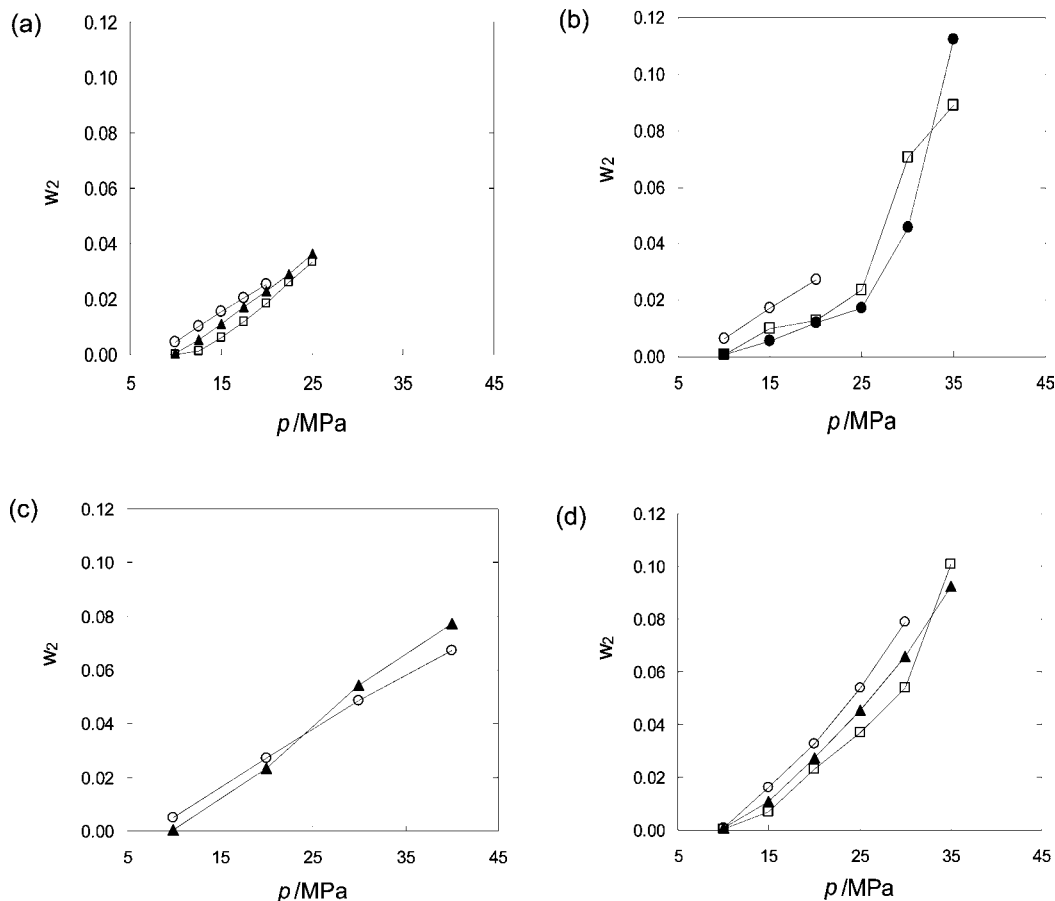


**Figure 3.** Temperature dependence of squalene solubility  $w_2$  in  $\text{SCCO}_2$  according to different sets of data: (a) refs 4 and 5; (b) ref 10; (c) ref 11; (d) this work. Symbols:  $\circ$ ,  $T = 313 \text{ K}$ ;  $\blacktriangle$ ,  $T = 323 \text{ K}$ ;  $\square$ ,  $T = 333 \text{ K}$ ;  $\bullet$ ,  $T = 363 \text{ K}$ .

Although deviations between experimental and calculated compositions were not reported in any of the works, a satisfactory representation of phase compositions could be observed in the pressure vs CO<sub>2</sub> weight fraction representations depicted in the corresponding works.

Despite the utilization of a separate set of parameters for each considered temperature, the procedure adopted to correlate the experimental data was not the usual. For example, Catchpole et al.<sup>4</sup> optimized the CO<sub>2</sub> *a* and *b* parameters of the PR-KM EoS at each temperature and pressure condition so that the density and fugacity/pressure ratio matched that predicted by the IUPAC equation of state for CO<sub>2</sub>. Using the SRK-MKP EoS, Brunner et al.<sup>10</sup> correlated saturated liquid densities and vapor pressures to fit pure component critical parameters and acentric factors: the resulted critical parameters for CO<sub>2</sub> (310.11 K and 8.28 MPa) were considerably higher than the real values (304.19 K and 7.38 MPa), and also exaggerated values for the squalene acentric factor ( $\omega = 1.9083$ ) resulted. These modeling results<sup>4,10</sup> suppose that the phase equilibria representation of the squalene + CO<sub>2</sub> system is not easy to be satisfactorily carried out.

In this work, the capability of a group contribution based model, namely, the GC-EoS, to represent the experimental data measured is evaluated. In previous works,<sup>13</sup> this model was satisfactorily utilized to represent phase equilibria of high molecular weight substances and SCCO<sub>2</sub>. However, in the case of squalene and using Catchpole et al.<sup>4,5</sup> experimental data, previous experience<sup>9</sup> demonstrated a problematic representation. Bearing in mind the discrepancies between previous data reported<sup>4,5</sup> and the data measured in this work, the GC-EoS modeling of the squalene + CO<sub>2</sub> system was attempted again to ascertain the capacity or deficiency of the model.

The Group Contribution Equation of State (GC-EoS) is based on the generalized van der Waals partition function and combines the group contribution principle with local-composition mixing rules. The model has two contributions to the residual Helmholtz energy of the system: a Carnahan–Starling type repulsive term and an attractive expression based on the group contribution approach. The GC-EoS repulsive term is modeled assuming hard sphere behavior for the molecules, and each substance is characterized by its critical hard sphere diameter *d<sub>c</sub>*. The attractive term is a group-contribution version of the NRTL model and has five pure-group parameters (*T\**, *q*, *g\**, *g'*, and *g''*) and four binary interaction parameters (*k<sub>ij</sub>*, *k'<sub>ij</sub>*,  $\alpha_{ij}$ , and  $\alpha_{ji}$ ). With regard to the pure group parameters *g\**, *g'*, and *g''* are adjustable (energy) parameters, while *T\** and *q* are not. *T\** is a reference temperature, and *q* is the group surface parameter. For a detailed description of the model, the reader is referred to Skjold-Jørgensen.<sup>14</sup>

The GC-EoS was previously employed to represent squalene + CO<sub>2</sub> vapor–liquid equilibria.<sup>9,11</sup> The parameters for the CH=C group and its interactions with CO<sub>2</sub> had been reported by Pusch et al.<sup>15</sup> but did not provide a satisfactory representation of experimental data as was demonstrated in the previous works. The original parameters<sup>15</sup> were obtained by using vapor–liquid binary data which include low molecular weight olefins, and thus it is reasonable that they provided only an approximate prediction of phase equilibria behavior of mixtures containing high molecular weight olefins such as squalene.

Therefore, new parameters were estimated<sup>9</sup> using the experimental data of Catchpole et al.,<sup>4,5</sup> and a considerable improvement of the vapor–liquid equilibria representation

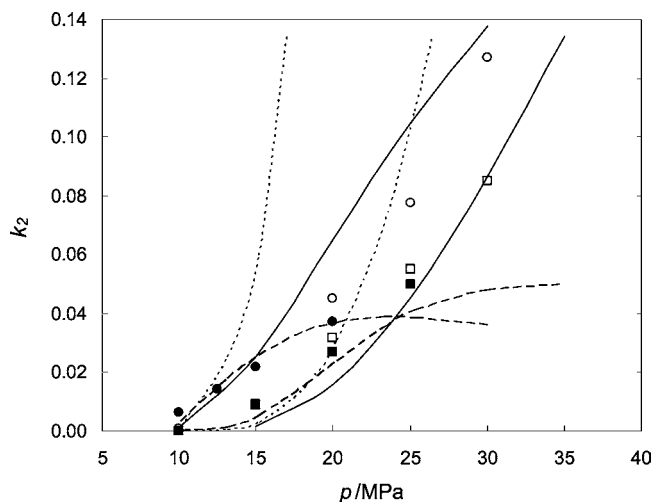


**Figure 4.** Squalene equilibrium constants ( $k_2 =$  mass fraction in supercritical phase/mass fraction in liquid phase):  $\circ$ , this work,  $T = 313$  K;  $\square$ , this work,  $T = 333$  K;  $\bullet$ , refs 4 and 5,  $T = 313$  K;  $\blacksquare$ , refs 4 and 5;  $T = 333$  K;  $-\cdot-$ , GC-EoS with original parameters;<sup>15</sup>  $-$ , GC-EoS with parameters regressed by Vázquez et al.;<sup>9</sup>  $-$ , GC-EoS with the new parameters regressed in this work.

**Table 3.** CO<sub>2</sub> (1) + Squalene (2) Phase Equilibria Modeling Using the GC-EoS Model: Pure Group and Binary Interaction Parameters Obtained Using Different Sets of Vapor–Liquid Phase Equilibria Data

Pure Group Parameters					
	reference temperature	group surface area	pure group energy parameters <sup>a</sup>		
	<i>T</i> */K	<i>q</i>	<i>g</i>	<i>g'</i>	<i>g''</i>
CH=C <sup>b</sup>	600.	0.676	546780.	-1.0966	0.0
CH=C <sup>c</sup>	600.	0.676	421650.	-1.3756	0.0
CH=C <sup>d</sup>	600.	0.676	510000.	-1.6379	-0.0416
Binary Group Interaction Parameters					
<i>i</i>	<i>j</i>	attractive energy parameters		nonrandomness parameters	
		<i>k<sub>ij</sub></i>	<i>k'<sub>ij</sub></i>	$\alpha_{ij}$	$\alpha_{ji}$
CO <sub>2</sub>	CH=C <sup>b</sup>	1.057	0.0	0.0	0.0
	CH=C <sup>c</sup>	0.882	0.022	-14.25	-14.25
	CH=C <sup>d</sup>	0.9831	0.235	-7.91	2.50
CH <sub>2</sub> /CH <sub>3</sub>	CH=C <sup>d</sup>	1.0488	-0.033	-4.12	-5.58

<sup>a</sup> cm<sup>6</sup>·atm·mol·(surface area segment)<sup>-2</sup>. <sup>b</sup> Original parameters.<sup>15</sup> <sup>c</sup> Parameters regressed by Vázquez et al.<sup>9</sup> <sup>d</sup> Parameters regressed in this work.

was achieved. Nevertheless, extrapolation of calculations at pressures higher than those employed in the regression procedure, that is (10 to 25) MPa, does not provide satisfactory results (see Figure 4).

In a recent contribution, Martínez-Correa et al.<sup>11</sup> demonstrated that the VLE representation of the squalene + CO<sub>2</sub> system using the GC-EoS model is influenced by the energy parameters and profoundly by the value of the critical hard sphere diameter *d<sub>c</sub>* of squalene (the particular values of squalene critical temperature and pressure showed no marked differences). Nevertheless, none of the different combinations of energy parameters (CH=C pure group and CH=C vs CO<sub>2</sub> binary interaction) and squalene *d<sub>c</sub>* value employed could reproduce both qualitatively and quantitatively the solubility of squalene in CO<sub>2</sub> up to pressures around 40 MPa.<sup>11</sup>

In this work, group parameters and squalene critical parameters (*T<sub>c</sub>* and *d<sub>c</sub>*) were simultaneously regressed using the

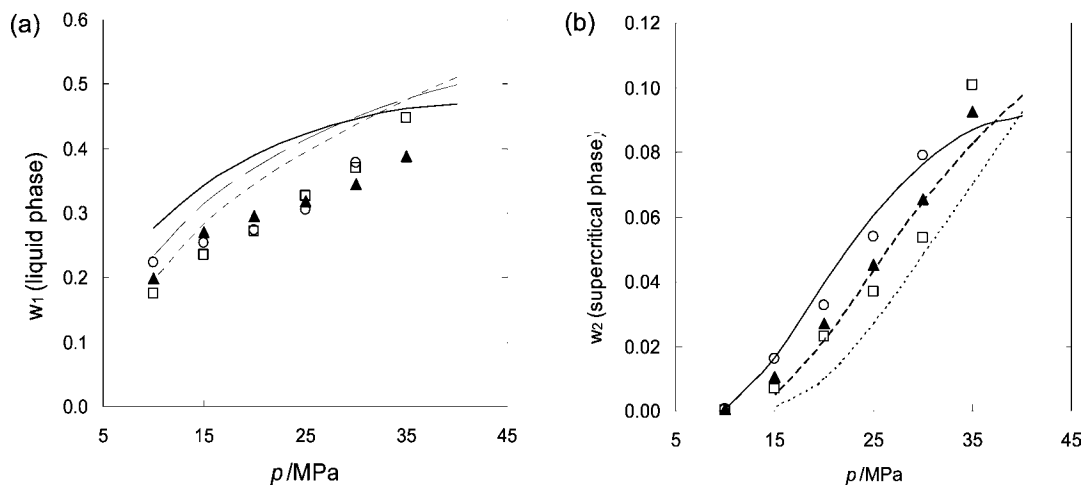


**Figure 5.** Squalene + CO<sub>2</sub> phase equilibria: (a) CO<sub>2</sub> mass fraction  $w_1$  in liquid phase and (b) squalene mass fraction  $w_2$  in supercritical phase. Data measured in this work: ○,  $T = 313$  K; ▲,  $T = 323$  K; □,  $T = 333$  K. GC-EoS representation using the parameters regressed in this work: - - -,  $T = 333$  K; — —,  $T = 323$  K; —,  $T = 313$  K.

experimental data given in Table 1. Squalene critical pressure ( $P_c$ ) was calculated according to the equation given by Skjold-Jørgensen:<sup>13</sup>  $d_c = (0.08943RT_c/P_c)^{1/3}$ . The squalene critical values resulted to be  $T_c = 828$  K,  $P_c = 8.9$  bar, and  $d_c = 8.845$  cm $\cdot$ mol<sup>-1</sup>, which are in accordance with the different sets presented by Martínez-Correa et al.<sup>11</sup> The optimal values obtained for the group energy parameters are given in Table 3 and are compared with the parameters regressed in previous works<sup>9,15</sup> and with those employed by Martínez-Correa et al.<sup>11</sup>

Figure 4 and Figure 5 show that the new GC-EoS parameters can provide a much better squalene + CO<sub>2</sub> phase equilibria representation in comparison with previous parameters reported. Nevertheless, it has to be pointed out that the improvement obtained in this work has been achieved due to the introduction of binary interaction parameters between the paraffin (CH<sub>2</sub>, CH<sub>3</sub>) and olefin (CH=C) groups. That is, like in previous works<sup>9,11</sup> when the CH=C pure group and the olefin-CO<sub>2</sub> or paraffin-CO<sub>2</sub> interactions were considered as optimization parameters, no satisfactory representation could be obtained.

The introduction of nonideal paraffin-olefin binary interaction parameters is not a usual procedure adopted in group contribution based models and should be interpreted as a deficiency of the model, considering further the low number of functional groups involved in the squalene + CO<sub>2</sub> system. Nevertheless, it is recognized that the quality of the GC-EoS predictions decreases as the complexity and/or size of the molecules are severely increased.<sup>14</sup> Further, the model should not be expected to be very accurate at pressures above (25 to 30) MPa, owing to the bad representation of total as well as partial liquid volumes.<sup>14</sup> Several works<sup>11,13,16</sup> confirmed these deficiencies and solved them utilizing a particular parametrization procedure, applicable only to the case of high size-asymmetric systems. In this work, a reasonable GC-EoS representation of squalene + CO<sub>2</sub> phase compositions up to pressures around 40 MPa could only be obtained by introducing nonideal energy interactions between the paraffin and olefin functional groups.

## Conclusions

New experimental vapor-liquid equilibria data of the binary squalene + CO<sub>2</sub> mixture were reported at pressures ranging from (10 to 35) MPa and at  $T = (313, 323, \text{ and } 333)$  K. The compositions measured were compared with previous data available in the literature. Reasonably average relative deviations

(ARD) were obtained with respect to the data reported by Brunner et al.:<sup>10</sup> 0.06 in the liquid phase CO<sub>2</sub> mass fractions and 0.27 in the squalene solubility determinations.

The new data obtained in this work were correlated using the GC-EoS. Previous work<sup>9,11</sup> attempted to provide satisfactory parameters (the CH=C pure group and the CO<sub>2</sub>-CH=C energy interactions), but no satisfactory representation could be obtained even in qualitative terms. In this work, a qualitative satisfactory representation was obtained by introducing energy interaction parameters between the paraffin (CH<sub>2</sub>, CH<sub>3</sub>) and olefin (CH=C) groups, which was habitually considered an ideal interaction. The validity of introducing nonideal paraffin-olefin interaction parameters in the phase equilibria modeling of the squalene + CO<sub>2</sub> system should be investigated considering the high-pressure phase equilibria modeling of systems comprising supercritical alkanes (methane, ethane, propane) and high molecular weight olefins.

## Literature Cited

- (1) Kelly, G. S. Squalene And Its Potential Clinical Uses. *Alternat. Med. Rev.* **1999**, *4*, 29–36.
- (2) Smith, T. J.; Yang, G. Y.; Seril, D. N.; Liao, J.; Kim, S. *Carcinogenesis* **1998**, *19*, 703–706.
- (3) Catchpole, O. J.; Kamp, J. V.; Grey, J. B. Extraction of Squalene from Shark Liver Oil in a Packed Column Using Supercritical Carbon Dioxide. *Ind. Eng. Chem. Res.* **1997**, *36*, 4318–4324.
- (4) Catchpole, O. J.; Kamp, J. V. Phase Equilibrium for the Extraction of Squalene from Shark Liver Oil Using Supercritical Carbon Dioxide. *Ind. Eng. Chem. Res.* **1997**, *36*, 3762–3768.
- (5) Catchpole, O. J.; Grey, J. B.; Noermark, K. A. Solubility of Fish Oil Components in Supercritical CO<sub>2</sub> and CO<sub>2</sub> + Ethanol Mixtures. *J. Chem. Eng. Data* **1998**, *43*, 1091–1095.
- (6) Catchpole, O. J.; Grey, J. B.; Noermark, K. A. Fractionation of Fish Oils Using Supercritical CO<sub>2</sub> and CO<sub>2</sub> + Ethanol Mixtures. *J. Supercrit. Fluids* **2000**, *19*, 25–37.
- (7) Catchpole, O. J.; Simões, P.; Grey, J. B.; Nogueiro, E. M. M.; Carmelo, P. J.; Nunes da Ponte, M. Fractionation of lipids in a static mixer and packed column using supercritical carbon dioxide. *Ind. Eng. Chem. Res.* **2000**, *39*, 4820–4827.
- (8) Bondioli, P.; Mariani, C.; Lanzani, A.; Fedeli, E.; Muller, A. Squalene Recovery from Olive Oil Distillates. *JAACS* **1993**, *70*, 763–766.
- (9) Vázquez, L.; Torres, C. F.; Fornari, T.; Señoráns, J.; Reglero, G. Recovery of Squalene from Vegetable Oil Sources Using Counter-current Supercritical Carbon Dioxide Extraction. *J. Supercrit. Fluids* **2007**, *40*, 59–66.
- (10) Brunner, G.; Saure, C.; Buss, D. Phase Equilibrium of Hydrogen, Carbon Dioxide, Squalene, and Squalane. *J. Chem. Eng. Data* **2009**, *54*, 1598–1609.
- (11) Martínez-Correa, H. A.; André, D. A.; Kanehisa, S. L.; Cabral, F. A. Measurements and thermodynamic modeling of the solubility of

- squalene in supercritical carbon dioxide. *J. Food Eng.* **2010**, *96*, 43–50.
- (12) Hernández, E. J.; Mabe, G.; Reglero, G.; Señoráns, F. J.; Fornari, T. High pressure phase equilibria data for the pseudo-ternary mixture sunflower oil + ethanol + carbon dioxide. *J. Chem. Eng. Data* **2008**, *53*, 2632–2636.
- (13) Fornari, T. Revision and summary of the group contribution equation of state parameter table: Application to edible oil constituents. *Fluid Phase Equilib.* **2007**, *262*, 187–209.
- (14) Skjold-Jørgensen, S. Gas solubility calculations II. Application of a new group-contribution equation of state. *Fluid Phase Equilib.* **1984**, *16*, 317–351.
- (15) Pusch, J.; Schmelzer, J. Extension of the Group-Contribution Equation of State Parameter Matrix for the Prediction of Phase Equilibria Containing Argon, Ammonia, Propene and other Alkenes. *Ber. Bunsenges, Phys. Chem.* **1993**, *97*, 597–603.
- (16) Cismondi, M.; Mollerup, J.; Brignole, E. A.; Zabaloy, M. S. Modelling the high-pressure phase equilibria of carbon dioxide - triglyceride systems: A parameterization strategy. *Fluid Phase Equilib.* **2009**, *281*, 40–48.

Received for review March 8, 2010. Accepted August 6, 2010. The authors gratefully acknowledge the financial support from the Ministerio de Ciencia e Innovación of Spain, projects 25506 FUN-C-FOOD (CONSOLIDER-INGENIO 2010) and AGL2008-05655/ALI.

JE1001939